

Dynamical Downscaling of ERA-Interim Temperature and Precipitation for Alaska

PETER A. BIENIEK,* UMA S. BHATT,⁺ JOHN E. WALSH,* T. SCOTT RUPP,[#] JING ZHANG,[@]
JEREMY R. KRIEGER,[&] AND RICK LADER*

* *International Arctic Research Center, University of Alaska Fairbanks, Fairbanks, Alaska*

⁺ *Geophysical Institute and Department of Atmospheric Sciences, University of Alaska Fairbanks, Fairbanks, Alaska*

[#] *Scenarios Network for Alaska and Arctic Planning, University of Alaska Fairbanks, Fairbanks, Alaska*

[@] *Department of Physics and Department of Energy and Environmental Systems, North Carolina A&T State University, Greensboro, North Carolina*

[&] *Arctic Region Supercomputing Center, University of Alaska Fairbanks, Fairbanks, Alaska*

(Manuscript received 4 June 2015, in final form 27 October 2015)

ABSTRACT

The European Centre for Medium-Range Weather Forecasts interim reanalysis (ERA-Interim) has been downscaled using a regional model covering Alaska at 20-km spatial and hourly temporal resolution for 1979–2013. Stakeholders can utilize these enhanced-resolution data to investigate climate- and weather-related phenomena in Alaska. Temperature and precipitation are analyzed and compared among ERA-Interim, WRF Model downscaling, and in situ observations. Relative to ERA-Interim, the downscaling is shown to improve the spatial representation of temperature and precipitation around Alaska's complex terrain. Improvements include increased winter and decreased summer higher-elevation downscaled seasonal average temperatures. Precipitation is also enhanced over higher elevations in all seasons relative to the reanalysis. These spatial distributions of temperature and precipitation are consistent with the few available gridded observational datasets that account for topography. The downscaled precipitation generally exceeds observationally derived estimates in all seasons over mainland Alaska, and it is less than observations in the southeast. Temperature biases tended to be more mixed, and the downscaling reduces absolute bias at higher elevations, especially in winter. Careful selection of data for local site analysis from the downscaling can help to reduce these biases, especially those due to inconsistencies in elevation. Improved meteorological station coverage at higher elevations will be necessary to better evaluate gridded downscaled products in Alaska because biases vary and may even change sign with elevation.

1. Introduction

Climate change in Alaska has been well documented (Markon et al. 2012), and Alaska's geographical complexity requires high-resolution meteorological information to prepare for future changes. Spatial resolution is especially important in areas of significant topography and in coastal regions. Alaska's major topographic features include extensive coastlines, islands, and mountain ranges containing the tallest mountains in North America. Its economy depends heavily on oil and mineral extraction, fishing, and tourism, activities that are all intimately tied to weather and climate. The Arctic is also a militarily strategic location, and sea ice decline is expected to increase ship

traffic, leading to enhanced security risks (e.g., Knell 2008). Many Alaska residents depend on food obtained through hunting and gathering, the future of which is uncertain at present. All of these activities rely heavily on environmental information, especially historical observations and future projections. Climate projections of temperature, precipitation, and winds are especially important but must be at appropriate spatial and temporal resolution to be useful for future planning.

Climate information required for future planning is typically needed for regions around cities or villages that are smaller than the size of a global-model grid box (~100 km). The representation of the terrain is notably different in a 20-km regional model (Fig. 1a) versus a reanalysis product at ~100 km (Fig. 1b), and the model resolution impacts meteorological variables that are sensitive to topography. Since temperature and precipitation vary strongly with altitude, the improved representation of

Corresponding author address: Peter A. Bieniek, 930 Koyukuk Dr., P.O. Box 757340, Fairbanks, AK 99775.
E-mail: pbieniek@alaska.edu

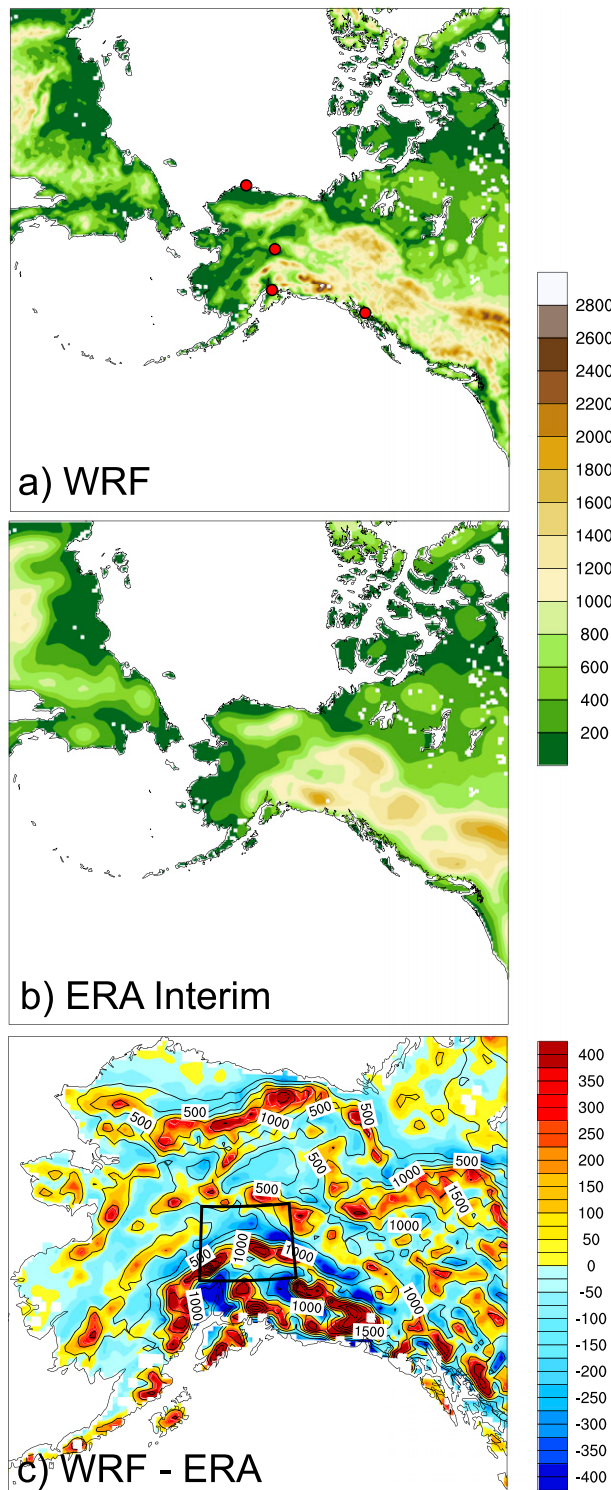


FIG. 1. Downscaling domain showing (a) WRF Model and (b) ERA-Interim topography (m). (c) The difference of surface elevations (m), WRF Model minus reanalysis topography, with a box denoting the areal coverage of Figs. 3 and 4. The locations of the four meteorological stations of this study are shown by the red dots in (a).

topography found with increasing model resolution enhances the simulation quality of these quantities (e.g., Fig. 4 in Bhatt et al. 2007). While dynamical downscaling has significantly larger computational overhead than statistical downscaling, one advantage is that the regional model output provides a full suite of dynamically consistent meteorological variables, allowing the investigation of mechanisms associated with a given behavior. Statistical downscaling also requires long observational records for training data, which are not always available for Alaska where many data voids exist. Nevertheless, each method has its strengths and weaknesses, as summarized below. The present study examines dynamical downscaling over the historical period to document biases in the simulations, investigate climatological patterns, and highlight the local detail that is added to the coarse reanalysis by the downscaling procedure over Alaska. This study focused on temperature and precipitation, as these are key variables in present climate science research activities. As background for the dynamical downscaling study presented here, we first assess the strengths and limitations of alternative approaches to downscaling.

Lessons learned from previous Alaska downscaling

Statistical downscaling has previously been conducted for Alaska with a focus on producing high-resolution monthly grids (<5-km grid increment) of temperature and precipitation. The Scenarios for Alaska and Arctic Planning (SNAP) at the University of Alaska Fairbanks has conducted statistical downscaling using the “delta” method to downscale monthly temperature and precipitation for more than 500 locations (communities) in Alaska and western Canada (https://www.snap.uaf.edu/sites/all/modules/snap_community_charts/charts.php). The delta method is similar to bias correction in which a model’s simulated future change from the present is simply added (as an adjustment or “delta”) to a high-resolution historical field of the same variable. The historical data providing the basis for the SNAP downscaling were from the Parameter-Elevation Regressions on Independent Slopes Model (PRISM) monthly climatology for Alaska (Simpson et al. 2005) at 2.0-km resolution (for downscaling of CMIP3 models) and 0.8 km (for downscaling of CMIP5 models). Monthly temperature and precipitation have also been downscaled using the delta method by Hill et al. (2015) who utilized PRISM as the baseline climatology, but anomaly fields were derived directly from station data and then interpolated using a spline with tension approach to a 2-km grid. These aforementioned downscaling products do not include daily output and are therefore not as useful for quantifying extreme events, which occur at daily or shorter time scales.

Statistical downscaling of daily temperature and winds has been undertaken at SNAP following the quantile-mapping method. The essence of the quantile-mapping method is the adjustment of each quantile (e.g., percentile or other segment of a distribution) of model output for a past period to match a corresponding distribution of target values for the same time period. The target values are typically observed values, or values from an observationally based reanalysis. SNAP has used quantile mapping of output from several CMIP5 models to project changes in the occurrences of extremes of temperature and wind speeds at various Alaskan coastal locations (http://shiny.snap.uaf.edu/temp_wind_events/). However, the validity of the historical wind data (in this case, from an atmospheric reanalysis) is a key limitation in this particular application of quantile mapping.

In the case of Alaska and elsewhere, applications of statistical downscaling are limited by the availability of the high-resolution observational data to compute the necessary statistics. Many variables such as wind, solar radiation, and evapotranspiration have limited gridded historical data that make statistical downscaling either impossible or questionable. Moreover, the increments of future change that are added to historical values in applications of the delta method are based on coarse-resolution global models and hence are unrealistically smooth. For these reasons, there are unique advantages to dynamical downscaling, which readily produces sub-daily products and does not require historical training data to develop statistics, as dynamical equations are used in the driving model.

There has been limited dynamical downscaling conducted for Alaska. Past studies have focused primarily on applications for estimating glacier mass balance (Zhang et al. 2007a,b), which used a high-resolution MM5 regional model (Grell et al. 1994) to dynamically downscale global climate model and reanalysis data. The downscaled temperatures and precipitation were used to estimate the mass balance for the Gulkana glacier in the Alaska Range and the Hubbard and Bering glaciers along the south coast of Alaska over the 1994–2004 period, and these estimates were validated against multiyear observations (Zhang et al. 2007a,b). Forcing of the glacier mass balance model revealed its sensitivity to biases in the temperature and precipitation values, which led to a process for correcting seasonal biases. Gulkana glacier mass balance calculated with the seasonally corrected downscaled variables compared favorably to the observed mass balance (Zhang et al. 2007b). The glacier studies demonstrated the value of dynamical downscaling for Alaska, although they highlighted the necessity of bias correction to produce

downscaled data of sufficient reliability to force glacial process models.

The Chukchi–Beaufort High-Resolution Atmospheric Reanalysis (CBHAR; Liu et al. 2014; Zhang et al. 2013) is a focused regional reanalysis conducted in northern Alaska and is related to dynamical downscaling. This reanalysis employed the WRF Model (Skamarock et al. 2008) and WRF Model data assimilation system (WRFDA; Huang et al. 2009; Barker et al. 2012) to produce a 31-yr, 10-km horizontal resolution, 1-hourly high-frequency regional reanalysis. The CBHAR reanalysis, particularly the surface wind field, demonstrates consistent improvements for every season of the year and four times (i.e., 0000, 0600, 1200, and 1800 UTC) of the day when compared with the European Centre for Medium-Range Weather Forecasts interim reanalysis (ERA-Interim), which was used to force the model (Zhang et al. 2013). The high temporal and spatial resolution CBHAR provides a unique opportunity to quantitatively study the mesoscale climatology and variability of the area's surface winds, including the sea breezes, up/downslope winds, and the mountain barrier jets in northern Alaska (Zhang et al. 2016). A broader downscaling/reanalysis effort was the Arctic System Reanalysis (ASR; Bromwich et al. 2016), which used the WRF Model for pan-Arctic downscaling of the NCEP–NCAR reanalysis. Its domain encompassed the entire Arctic with a grid increment of 30 km. The data from ASR are presently limited to 2000–12, but an extension to 1979 is under way. Our downscaling builds on the ASR, CBHAR, and MM5 study by providing data coverage to an Alaska-centered domain at 20 km, which is the highest spatial resolution available for any similar hourly observational data that covers the entire region of Alaska. The downscaling data presented in this paper were not produced with data assimilation as in ASR and CBHAR. However, spectral nudging was employed to constrain the simulation to the input ERA-Interim forcing data.

2. Data and methods

a. Downscaling procedure

The Advanced Research version of the WRF Model (Skamarock et al. 2008) was utilized to dynamically downscale data in this study. An optimized configuration of the WRF Model physical parameterizations for Alaska (Zhang et al. 2013) was employed. Nudging was used during the WRF Model simulations to ensure that the model did not deviate significantly from the input reanalysis forcing. Following Zhang et al. (2013), spectral nudging with a wavenumber of 3 and was applied to all variables at all vertical levels in the downscaling simulations. The WRF Model configuration for

TABLE 1. WRF Model configuration.

Options		Configuration
Physics	Microphysics	Morrison 2-moment
	Radiation	RRTM
	Cumulus	Grell 3D
	Planetary boundary layer	Mellor–Yamada–Janjić
	Surface layer	Monin–Obukhov
Grid	Land surface model	Noah land surface model
	Horizontal grid spacing	20 km
Nudging	Vertical levels	49 levels with top at 10 hPa
	Spectral nudging	All levels

this study is summarized in Table 1. The Morrison 2-moment (Morrison et al. 2009) microphysical and Grell 3D cumulus schemes were utilized to parameterize cloud and precipitation processes. Shortwave and longwave radiative effects were parameterized by the Rapid Radiative Transfer Model (RRTM) for GCMs (Iacono et al. 2008). Boundary layer and surface-layer processes utilized the Mellor–Yamada–Janjić (Janjić 1994) and Janjić eta (Monin–Obukhov) schemes, respectively. A thermodynamic sea ice model (Zhang and Zhang 2001) was coupled with the Noah land surface model used within the WRF Model to accurately model the thermal conditions over sea ice.

The downscaling covered a domain with 262×262 grid points that encompassed all of Alaska and portions of far eastern Russia and northern Canada at 20-km spatial resolution (Fig. 1a) with 49 vertical model levels. The downscaling simulations were integrated for a total 54 h after initialization at 48-h increments; each 54-h simulation includes 6 h of spinup time and 48 h of actual downscaled output. The model was reinitialized every two days where the first 6 h of spinup time data were discarded. These spinup data could be discarded because they overlap with the last 6 h of the previous 54-h integration. The output from the 2-day simulations was combined together to form the final downscaled product. Each initialization occurred at 1800 UTC (0900 Alaska standard time). Because the WRF Model is reinitialized every 2 days, parameters such as atmospheric moisture and energy are not precisely conserved over the entire period of the downscaling as in a continuous model run. Spectral nudging of the atmospheric fields was performed every 6 h. Hourly WRF Model output was saved and used to produce daily means, maximum and minimum values of downscaled variables. Post-processing of the WRF Model output was conducted using the Unified Post-Processing (UPP) software package. UPP was utilized to interpolate from the model sigma coordinates to 12 standard pressure levels (1000–50 hPa) for the upper-air variables.

b. Input and evaluation data

The reanalysis dataset known as ERA-Interim (Dee et al. 2011) was downscaled for the period 1979–2013 using the previously described WRF Model procedure for this study. The ERA-Interim data were obtained at 0.75° (~ 83 km) spatial and 6-hourly temporal resolution. The following variables were obtained to force the WRF Model downscaling: surface, 2-m and upper-air temperature, 10-m and upper-air u and v wind, 2-m and upper-air relative humidity, geopotential height of the pressure levels, mean sea level pressure, surface pressure, sea surface temperatures, sea ice concentration, soil temperature and moisture at four soil levels, snow depth, and snow density. A few minor data issues were corrected in the input data prior to downscaling, including several short periods with inhomogeneities in the 6-hourly sea ice concentration after 2000 (in those cases the data from the previous time step were used to replace the bad data frames). ERA-Interim was selected as it has been successfully downscaled using the WRF Model in many regions of the world (e.g., Gao et al. 2015; Srivastava et al. 2014, 2013; Soares et al. 2012), used in previous Arctic WRF Model simulations and analysis (e.g., Liu et al. 2014) and is among the best performing reanalysis datasets for Alaska (Lader et al. 2016) and the wider Arctic (Lindsay et al. 2014).

The downscaled data were compared with the original input reanalysis data and meteorological station data. Station temperature and precipitation were obtained from the Global Summary of the Day (GSOD) database maintained by the National Centers for Environmental Information (formerly National Climatic Data Center) for stations throughout Alaska, Canada, and Russia for 1979–2013. The GSOD database was selected because it uses a 0000 UTC instead of local midnight to compute daily maximum, minimum, and average temperatures. This manner of daily averaging is consistent with downscaled model parameters and results in a clean comparison between observations and the downscaled variables. Monthly gridded 2-km temperature and precipitation for 1979–2009 produced by Hill et al. (2015) were also utilized to augment station observations, as stations tend to be only at lower elevations with sparse coverage in many areas. Hill et al. (2015) statistically downscaled monthly temperature and precipitation using spline and tension interpolation of station anomalies to a regular grid followed by a delta-method adjustment using the PRISM 1971–2000 climatology (Simpson et al. 2005) as the baseline data to form the final product. These gridded temperature and precipitation data (herein called gridded observations) were bilinearly interpolated to the 20-km WRF Model

grid for ease of comparison. Solar radiation data were obtained from the U.S. Department of Energy's Atmospheric Radiation Measurement (ARM) Program observation site at Barrow (available online at <http://www.archive.arm.gov>). The downscaled data were evaluated using two methods: bias (i.e., the difference in means) and root-mean-square error (RMSE; Wilks 2006). Station and reanalysis data contain their own uncertainties; therefore the term "bias" is used only to denote the difference between the WRF Model output and observational data, not to imply that the differences are entirely errors in the model results.

3. Results

a. Evaluation of temperature and precipitation

Dynamical downscaling adds value by enhancing local information through the inclusion of mesoscale atmospheric features, especially in regions with complex topography like Alaska. The difference between the WRF Model and reanalysis terrain is quite large throughout Alaska (Fig. 1c). The mountains in the WRF Model are often more than 200 m taller than those in the reanalysis in the major mountain ranges. Likewise, the WRF Model topography is frequently more than 100 m lower in elevation than the reanalysis in many of the major valleys. These differences are largely due to the unrealistically smooth topography in the reanalysis over the Alaska domain (cf. Figs. 1a and 1b). These disparities in the terrain account for some of the differences between the reanalysis and the downscaled temperature and precipitation that will be shown next.

The spatial complexity of temperature and precipitation can be seen by examining the maximum of the eight RMSEs of the monthly time series of each center grid point in comparison with its eight neighboring points (Fig. 2), thereby highlighting the similarity of each grid point with its adjacent points. Lower RMSEs indicate that the grid point was more similar to its neighbors. For temperature (Fig. 2a), grid similarity is lowest in the mountainous regions of south-central and southeast Alaska and also at the land-sea boundary, which stands out as a band of higher RMSEs outlining the entire coastline. For precipitation (Fig. 2b), grid similarity is lowest in mountainous terrain. The same calculation was also performed on the input reanalysis bilinearly interpolated to the WRF Model grid and then subtracted from the downscaled result. Grid similarity is reduced for both temperature and precipitation relative to the original reanalysis (Figs. 2c,d), especially in the mountainous terrain of south-central and southeast Alaska. Reduced grid similarity indicates that local

atmospheric features were added by the WRF Model to the downscaled output, which should improve temperature and precipitation fields in the complex terrain of Alaska. Such improvements in south-central and southeast Alaska are especially valuable as the majority of the population lives in these areas.

A significant improvement in the spatial representation of 2-m temperature in the downscaling compared to the coarse reanalysis is seen in a comparison with gridded observed seasonal climatologies for 1979–2009 (Fig. 3). Here the climatological temperatures are compared in the Fairbanks vicinity (see box outlining the region in Fig. 1c), which is a region of complex topography with the Alaska Range running east–west across the southern portion of each panel in Fig. 3. This region also includes the highest-elevation point in North America, Mount McKinley (Denali), which is located in the southwest corner of each panel in Fig. 3. The reanalysis has a much smoother climatological temperature gradient in all seasons, with little indication of the topography in the region (Figs. 3a–c), while the downscaling (Figs. 3e–h) has a signature similar to the gridded observations (Figs. 3i–l). In winter (Figs. 3a,e,i) the reanalysis has a smooth north–south temperature gradient with little hint of the influence of the mountains in the contours (Fig. 3a), whereas the downscaling has warmer 2-m temperatures over the higher terrain relative to lower elevations (Fig. 3e). The downscaled temperatures are more similar to observations (Fig. 3i) and consistent with the frequent presence of low-level temperature inversions in the area. A similar improvement in the spatial distribution of 2-m temperatures can be seen during spring (Figs. 3b,f,j), summer (Figs. 3c,g,k), and fall (Figs. 3d,h,l) when the mountainous regions are much cooler than the surroundings in the downscaled and observed data than in the reanalysis.

Comparisons of the climatologies of seasonal precipitation reveal a similar improvement of the spatial distribution around complex topography in the downscaled versus the reanalysis data (Fig. 4). In all seasons precipitation amounts are larger over the mountains in the downscaling (Fig. 4e–h) when compared to the reanalysis (Figs. 4a–d), which shows only a smooth gradient. The enhanced precipitation over the mountains in the downscaling (Figs. 4e–h) is more spatially consistent with gridded observations (Figs. 4i–l) in all seasons. Improved spatial representation of temperature and precipitation is a key improvement added to the coarse reanalysis by dynamical downscaling for Alaska.

Because correlations with data from single stations are sensitive to details of the station location, we also compared the downscaled output with regionally

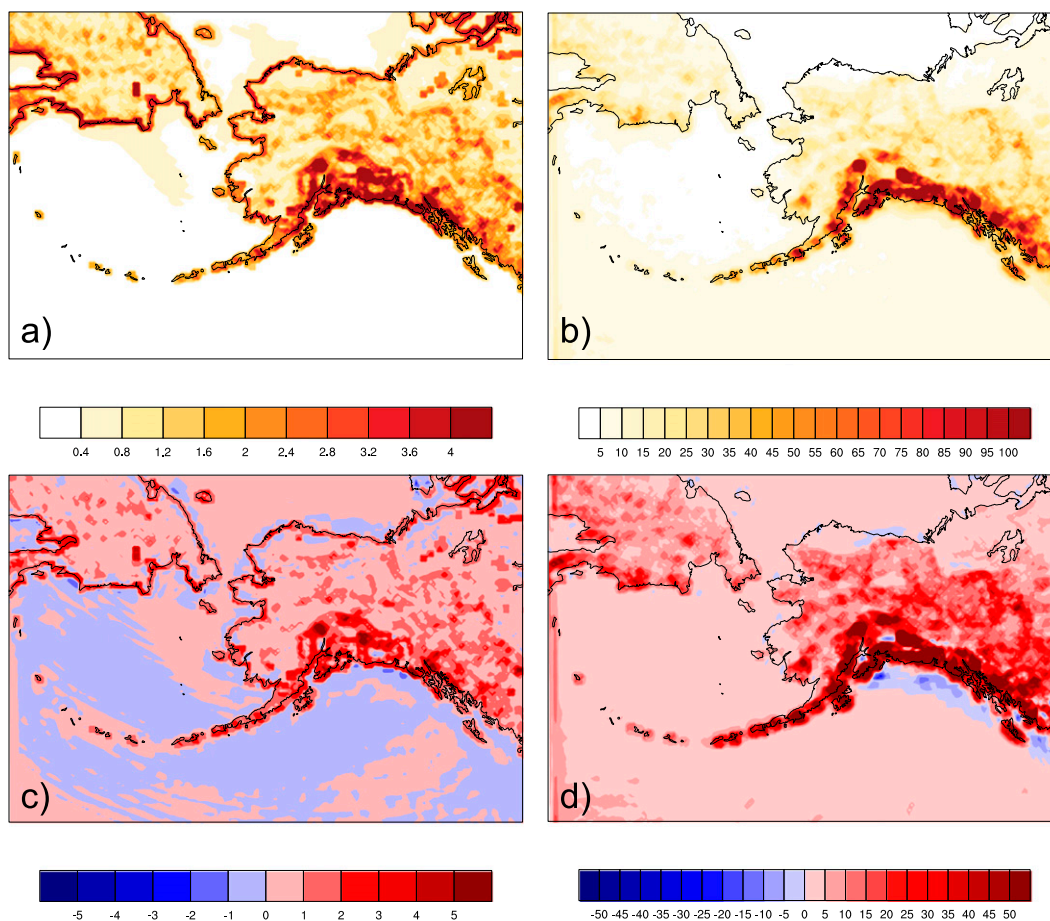


FIG. 2. The similarity of each grid point to its neighbors of monthly downscaled (a) 2-m temperature ($^{\circ}\text{C}$) and (b) precipitation (mm). The differences (downscaled minus ERA-Interim) interpolated to the downscaled grid for (c) 2-m temperature ($^{\circ}\text{C}$) and (d) precipitation (mm). The similarity was determined by the maximum of the eight RMSEs of the monthly time series of each center grid point vs its eight neighboring points.

averaged downscaled temperatures based on Alaska's 13 climate divisions (Fig. 5). This comparison produced mixed results when compared with the coarse reanalysis and the gridded observations (Table 2). The Alaska climate divisions represent regions of homogeneous climate variability (Bieniek et al. 2012) and have been used to analyze climatic trends and variability (e.g., Bieniek et al. 2014; McAfee et al. 2014) and evaluate model/reanalysis performance (e.g., Lader et al. 2016). The downscaled temperatures have mixed positive and negative biases in all seasons and divisions when compared with the gridded observations, with the largest-magnitude departure of -3.1°C in the northeast gulf division in June–August (JJA). Correlations between regionally averaged downscaled seasonal values and corresponding (same division) observations are mostly greater than 0.9 with some exceptions such as the central panhandle divisions, which have a correlation of 0.58 in September–November (SON). RMSEs in all

regions are mostly less than 1.0°C with the largest RMSE of 3.1°C in the northeast gulf divisions (also the region with the greatest bias value) in June–August. When compared with similar metrics of bias, correlation, and RMSE of the reanalysis versus observations to assess the performance of the downscaling, the downscaling had mixed results. Overall, correlations were slightly higher or nearly the same as those of the reanalysis. Bias and RMSE in the downscaled output were lower in December–February (DJF) but higher in March–May (MAM) and JJA when compared with the values from the reanalysis.

A similar analysis of downscaled precipitation versus observations (Table 3) shows a general wet bias in all climate divisions north of the Alaska Range in most seasons, with a dry bias in the southern coastal divisions. The largest biases and RMSEs occur in the southern coastal divisions where precipitation amounts are typically much higher throughout the year than the northern

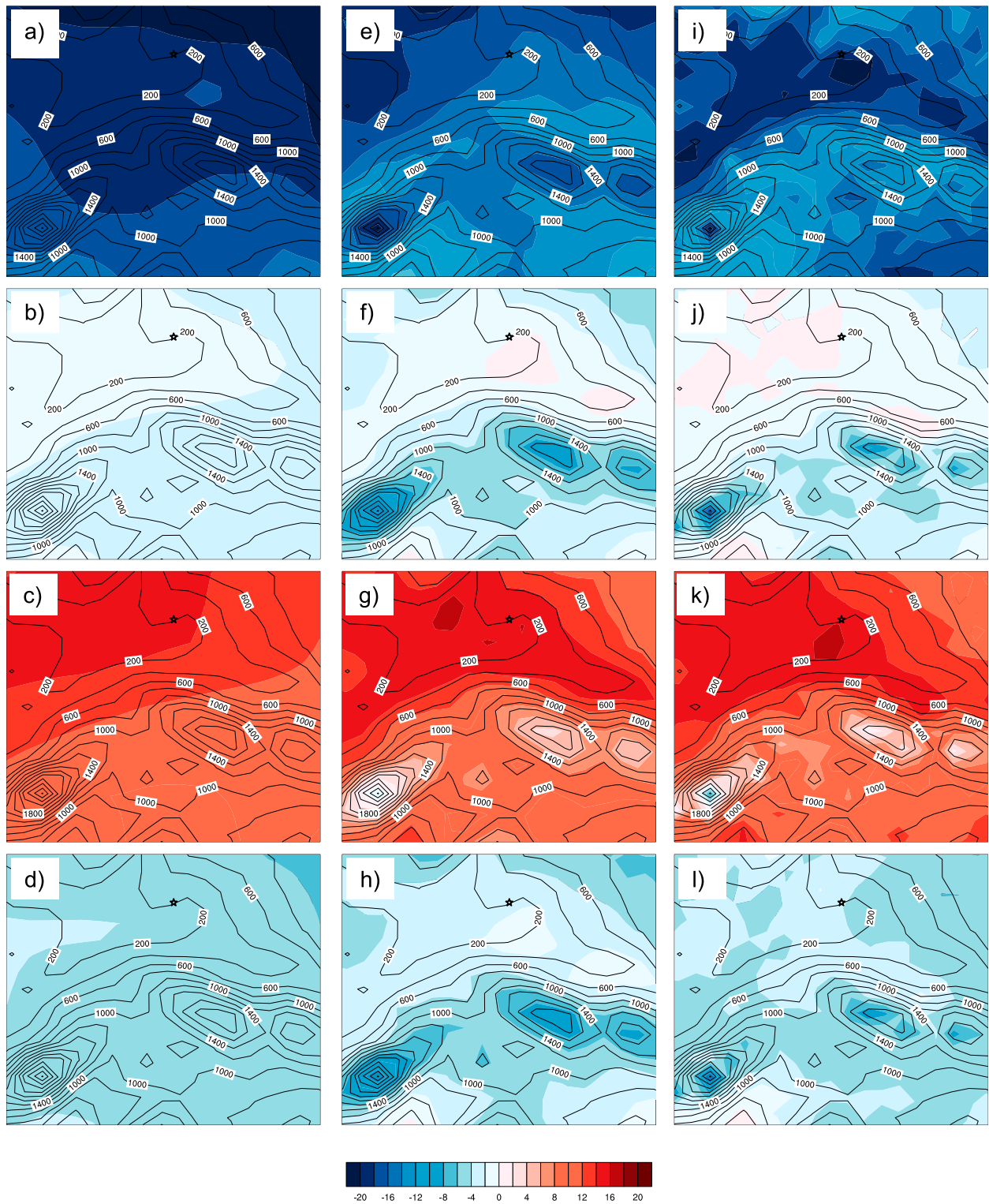


FIG. 3. (a)–(d) ERA-Interim, (e)–(h) downscaled, and (i)–(l) gridded observation seasonal average temperature climatologies (°C) for 1979–2009 with WRF Model topography (m) contours overlaid. The seasons analyzed were (top) DJF, (top middle) MAM, (bottom middle) JJA, and (bottom) SON. Fairbanks is shown by the star.

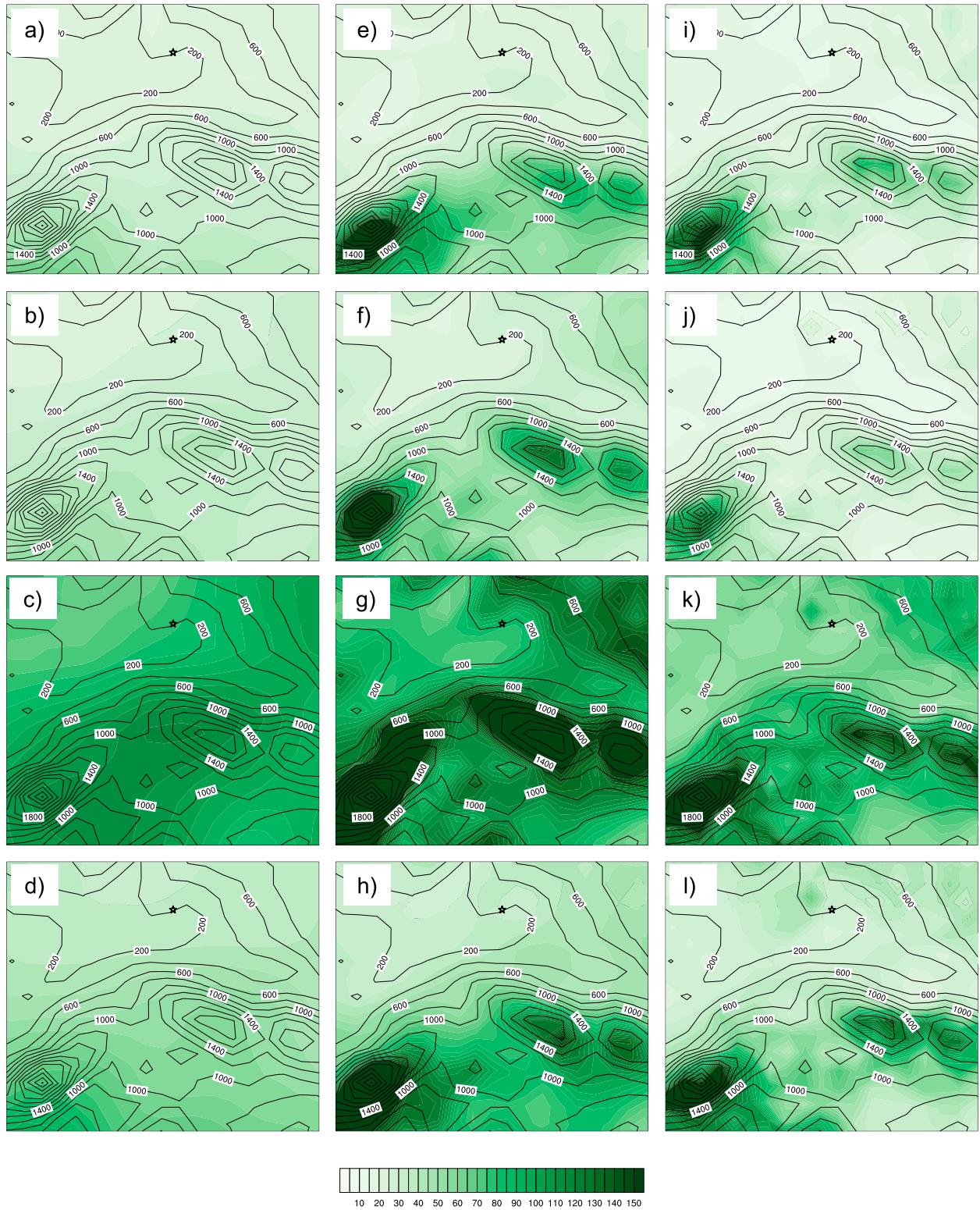


FIG. 4. As in Fig. 3, but for precipitation (mm).

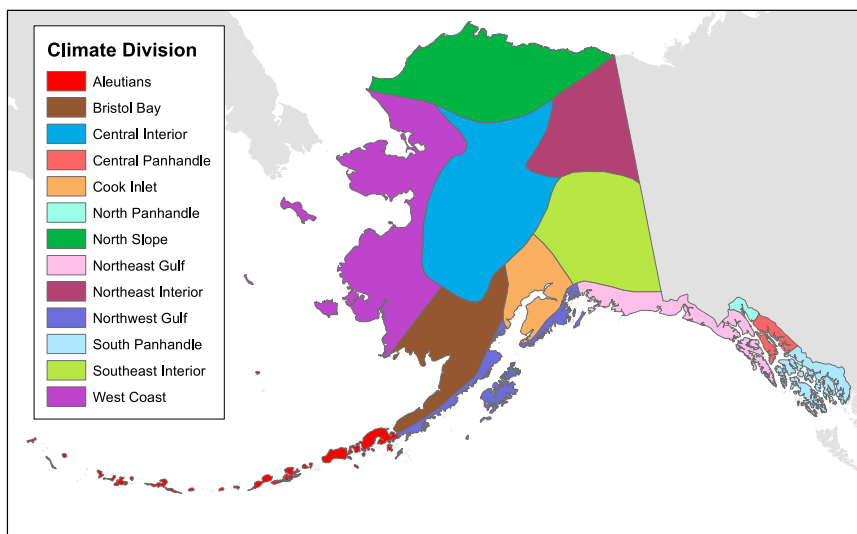


FIG. 5. The 13 Alaska climate divisions (Bienie et al. 2012) utilized for the analysis in Tables 2 and 3.

divisions (Bienie et al. 2012). Correlations of downscaled precipitation versus observations reveal lower correlations overall than for downscaled temperature compared to reanalysis. When compared with the same results for the reanalysis versus the observations, the northern climate divisions had larger wet biases in all seasons in the downscaled case than in the reanalysis. However, biases and RMSEs were generally reduced by the downscaling in the southern coastal divisions with some exceptions in the south panhandle and northwest gulf divisions where biases increased.

Improvements made by the downscaling in the spatial representation of temperature and precipitations over terrain shown in Figs. 3 and 4 are not evident in this comparison based on averages over larger regions. Accordingly, a direct grid-to-grid comparison is presented next in order to better assess local improvements that result from downscaling ERA-Interim. Local biases are evaluated by comparing seasonally averaged 2-m temperature from downscaling and station observations by subtracting the station data from the nearest adjacent downscaled grid point with the most similar elevation (Figs. 6a–d). For DJF, the downscaling was warmer than observations throughout much of Alaska with the exception of the northwest coastal regions, which were slightly cooler (Fig. 6a). At many stations in the interior, the downscaling had a warm bias reaching or exceeding 5°C in winter. This seems to indicate a warm bias in the model in winter; however, since most stations are at low elevations, making simple comparisons is somewhat problematic. Even with corrections in place for elevation it is possible that the elevation difference between

the stations and model accounts for this apparent DJF warm bias in the downscaling. The difference or bias was less pronounced and more mixed in MAM, JJA, and SON (Figs. 6b–d). The largest bias outside of winter was a cold bias during summer in the south-central coastal mountains of Alaska, approaching -6°C at several stations.

When the downscaled data were compared with gridded observations over Alaska, similar features to the station comparison are apparent (Figs. 6e–h). Low-elevation warm biases are evident in winter with cold biases over higher elevations throughout the state (Fig. 6e). These elevation-specific biases highlight the need to include high-altitude observations in generating and evaluating gridded data in mountainous regions. Cold biases occur in higher terrain throughout the interior in spring (Fig. 6f), again mostly at higher elevations. In summer and fall (Figs. 6g,h) warm biases are evident over lower elevations with cold biases over higher elevations. The southeast panhandle displays mainly weak warm biases in all seasons with slight cold biases over the mountains on the eastern side of the region.

The difference in the absolute value (herein referred to as absolute bias) of the downscaled bias and reanalysis bias (both compared to the gridded observations) was calculated for all seasons (Figs. 6i–l) to assess whether the biases were improved by the downscaling compared to the reanalysis. A negative value of this difference indicates that the downscaling had a smaller absolute bias than the reanalysis when both were compared with observations. It does not account for changes in the sign of the bias. The downscaling achieved the

TABLE 2. Bias, correlation, and RMSE of seasonal 2-m temperature for downscaled vs gridded observations and reanalysis vs gridded observations over the 13 Alaska climate divisions.

	Downscaled				Reanalysis			
	DJF	MAM	JJA	SON	DJF	MAM	JJA	SON
Bias (°C)								
North Slope	0.9	0.2	0.8	0.4	-1.6	-0.5	0.3	-0.3
West coast	-0.2	-0.2	0.4	-0.1	-0.4	0.0	0.0	-0.1
Central interior	0.5	-1.3	0.1	0.2	-0.2	-0.3	0.0	0.1
Northeast interior	-0.2	-1.9	0.3	0.3	-2.2	-1.5	0.0	-0.4
Southeast interior	1.4	-0.8	-1.2	0.3	-2.1	0.2	0.3	-0.3
Cook Inlet	0.5	-1.2	-1.6	-0.5	-2.2	-0.2	0.4	-0.6
Bristol Bay	0.0	-0.3	0.5	-0.1	-0.3	0.2	0.6	0.2
Northwest gulf	0.1	-0.7	-0.4	-0.2	1.2	0.5	0.4	1.2
Northeast gulf	0.7	-1.0	-3.1	-0.7	0.0	0.5	0.3	0.6
North panhandle	-0.2	-1.9	-2.6	-1.2	-4.0	-1.5	-0.4	-2.0
Central panhandle	0.8	0.2	1.4	0.8	-1.4	0.5	1.7	0.0
South panhandle	0.3	-0.1	0.3	0.6	-0.5	0.0	0.3	0.2
Aleutians	2.3	0.4	-0.4	1.0	4.2	1.8	0.0	2.5
Statewide	0.4	-0.7	-0.1	0.1	-0.9	-0.2	0.2	-0.1
Correlation								
North Slope	0.95	0.96	0.87	0.95	0.91	0.92	0.86	0.96
West coast	0.99	0.99	0.96	0.99	0.99	0.99	0.97	0.99
Central interior	0.93	0.94	0.83	0.97	0.91	0.95	0.86	0.96
Northeast interior	0.82	0.93	0.83	0.92	0.78	0.94	0.80	0.92
Southeast interior	0.96	0.97	0.94	0.97	0.95	0.98	0.92	0.99
Cook Inlet	0.98	0.97	0.94	0.98	0.98	0.96	0.94	0.97
Bristol Bay	1.00	0.98	0.95	0.98	1.00	0.99	0.97	0.99
Northwest gulf	0.99	0.96	0.95	0.95	0.99	0.97	0.93	0.95
Northeast gulf	0.96	0.96	0.96	0.97	0.94	0.94	0.93	0.96
North panhandle	0.95	0.93	0.80	0.94	0.89	0.90	0.78	0.92
Central panhandle	0.78	0.83	0.89	0.58	0.71	0.79	0.85	0.60
South panhandle	0.94	0.86	0.93	0.93	0.87	0.79	0.92	0.89
Aleutians	0.97	0.97	0.93	0.92	0.96	0.96	0.93	0.90
Statewide	0.98	0.98	0.93	0.99	0.98	0.98	0.93	0.99
RMSE (°C)								
North Slope	1.1	0.7	1.0	0.7	1.8	1.2	0.6	0.7
West coast	0.4	0.4	0.5	0.2	0.6	0.3	0.3	0.3
Central interior	1.0	1.4	0.6	0.5	1.0	0.6	0.5	0.5
Northeast interior	1.3	2.0	0.7	0.8	2.6	1.6	0.6	0.8
Southeast interior	1.5	0.9	1.3	0.6	2.2	0.4	0.5	0.5
Cook Inlet	0.7	1.2	1.6	0.6	2.2	0.4	0.5	0.8
Bristol Bay	0.3	0.5	0.6	0.3	0.3	0.3	0.6	0.3
Northwest gulf	0.3	0.7	0.5	0.4	1.2	0.6	0.5	1.3
Northeast gulf	0.8	1.1	3.1	0.7	0.7	0.6	0.4	0.7
North panhandle	0.6	1.9	2.6	1.3	4.2	1.6	0.7	2.1
Central panhandle	1.3	0.7	1.5	1.4	2.0	0.9	1.8	1.2
South panhandle	0.5	0.5	0.4	0.7	0.9	0.6	0.4	0.5
Aleutians	2.3	0.6	0.5	1.0	4.2	1.9	0.2	2.6
Statewide	0.5	0.7	0.3	0.3	1.0	0.3	0.4	0.2

greatest reduction in absolute bias in winter (Fig. 6i) over higher-elevation regions throughout Alaska. This was also the time when the downscaling had the biggest increase in biases compared with the reanalysis in the lower-elevation regions of eastern interior Alaska, where biases were approaching 6°C (Figs. 6a,e). These enhanced winter biases at low elevations may be related to shortcomings in how inversions are represented by the WRF Model in the exceptionally stable boundary

layer conditions that occur in the valley regions of interior Alaska in winter (Mölders and Kramm 2010). The differences between the biases in temperature downscaling versus reanalysis are much smaller in the remaining seasons of spring, summer, and fall (Figs. 6j-l). The exception is an isolated area of larger bias in the downscaling in summer in south-central Alaska (Fig. 6k). This issue is related to a cold bias induced by excessive snow remaining throughout the summer in the

TABLE 3. Bias, correlation and RMSE of seasonal precipitation for downscaled vs gridded observations and reanalysis vs gridded observations over the 13 Alaska climate divisions.

	Downscaled				Reanalysis			
	DJF	MAM	JJA	SON	DJF	MAM	JJA	SON
Bias (mm)								
North Slope	5.5	7.1	14.4	7.6	3.2	5.2	10.2	4.1
West coast	11.6	12.2	9.4	6.6	9.3	9.2	8.0	5.0
Central interior	12.7	18.7	32.2	12.4	8.7	12.2	15.0	8.7
Northeast interior	6.1	10.5	33.3	8.2	3.5	7.3	21.9	5.2
Southeast interior	16.7	25.9	27.5	20.3	7.2	11.7	9.4	6.4
Cook Inlet	28.8	27.3	9.5	9.1	9.4	13.8	2.4	-5.6
Bristol Bay	37.1	23.4	8.2	14.3	29.7	21.9	2.1	10.0
Northwest gulf	-24.7	-23.1	-22.2	-62.6	-75.4	-50.7	-41.6	-108.8
Northeast gulf	-147.5	-102.6	-153.3	-275.1	-149.6	-108.3	-144.9	-261.9
North panhandle	-21.8	23.9	0.2	-47.4	-67.7	-4.1	1.8	-70.7
Central panhandle	-197.3	-109.1	-128.5	-333.6	-219.0	-125.2	-135.3	-342.8
South panhandle	-142.5	-93.4	-65.6	-192.1	-116.0	-76.8	-59.8	-160.9
Aleutians	-28.4	-18.2	-34.4	-59.0	-50.5	-33.7	-38.0	-71.8
Statewide	-0.9	5.5	6.9	-13.8	-7.1	-0.6	-1.8	-18.8
Correlation								
North Slope	0.56	0.84	0.68	0.81	0.60	0.82	0.72	0.82
West coast	0.90	0.82	0.68	0.90	0.90	0.85	0.75	0.92
Central interior	0.93	0.85	0.65	0.96	0.92	0.87	0.75	0.96
Northeast interior	0.74	0.51	0.58	0.67	0.71	0.54	0.60	0.76
Southeast interior	0.81	0.52	0.80	0.86	0.80	0.62	0.79	0.86
Cook Inlet	0.75	0.70	0.71	0.88	0.76	0.70	0.79	0.90
Bristol Bay	0.62	0.76	0.39	0.75	0.63	0.75	0.49	0.81
Northwest gulf	0.89	0.90	0.73	0.83	0.92	0.89	0.76	0.88
Northeast gulf	0.88	0.85	0.92	0.92	0.88	0.87	0.92	0.92
North panhandle	0.67	0.81	0.79	0.90	0.77	0.85	0.79	0.94
Central panhandle	0.70	0.82	0.71	0.82	0.69	0.84	0.76	0.85
South panhandle	0.88	0.88	0.89	0.92	0.90	0.90	0.92	0.92
Aleutians	0.70	0.71	0.33	0.66	0.68	0.62	0.25	0.64
Statewide	0.92	0.89	0.66	0.94	0.93	0.91	0.78	0.95
RMSE (mm)								
North Slope	6.9	7.5	16.6	9.3	4.9	5.7	12.7	5.9
West coast	12.6	13.4	13.1	9.7	10.3	10.3	11.4	8.3
Central interior	13.4	19.5	34.3	13.1	9.4	12.9	18.1	9.6
Northeast interior	6.8	11.5	34.6	9.6	4.6	8.5	23.7	6.7
Southeast interior	18.1	27.3	29.4	21.8	9.7	13.3	14.3	9.7
Cook Inlet	34.8	32.7	21.8	20.3	19.4	21.1	17.8	17.2
Bristol Bay	39.8	26.3	19.4	22.1	32.5	24.9	16.6	18.0
Northwest gulf	33.6	29.0	27.6	69.0	80.1	54.9	43.6	113.2
Northeast gulf	159.7	108.4	157.1	282.9	161.8	113.5	149.0	270.1
North panhandle	50.4	32.0	18.8	58.2	79.2	20.0	18.6	77.9
Central panhandle	206.8	120.6	139.0	348.2	227.9	135.4	145.0	356.4
South panhandle	147.6	99.0	70.6	196.7	121.0	82.1	64.0	165.6
Aleutians	36.9	27.5	42.0	64.1	56.9	40.9	45.3	76.4
Statewide	4.1	6.9	10.3	14.9	7.9	3.3	6.8	19.6

input reanalysis as this is flagged as a glaciated region in ERA-Interim and given a fixed, unphysically high value of snow depth (Drusch et al. 2004). Snow cover and depth should be evaluated and improved in future Alaska dynamical downscaling activities that utilize reanalysis datasets.

Precipitation from the reanalysis is not initialized in the WRF Model; only the atmospheric humidity is ingested into the WRF Model from the reanalysis.

Therefore, the downscaled precipitation is generally a product of the WRF Model simulation. A comparison of the downscaled precipitation with station observations (Figs. 7a–d) shows a general wet bias at many stations in the regions that were climatologically the wettest during each season. This wet bias is not completely uniform as there are stations with strong dry biases adjacent to ones with strong wet biases in southeast Alaska. When the

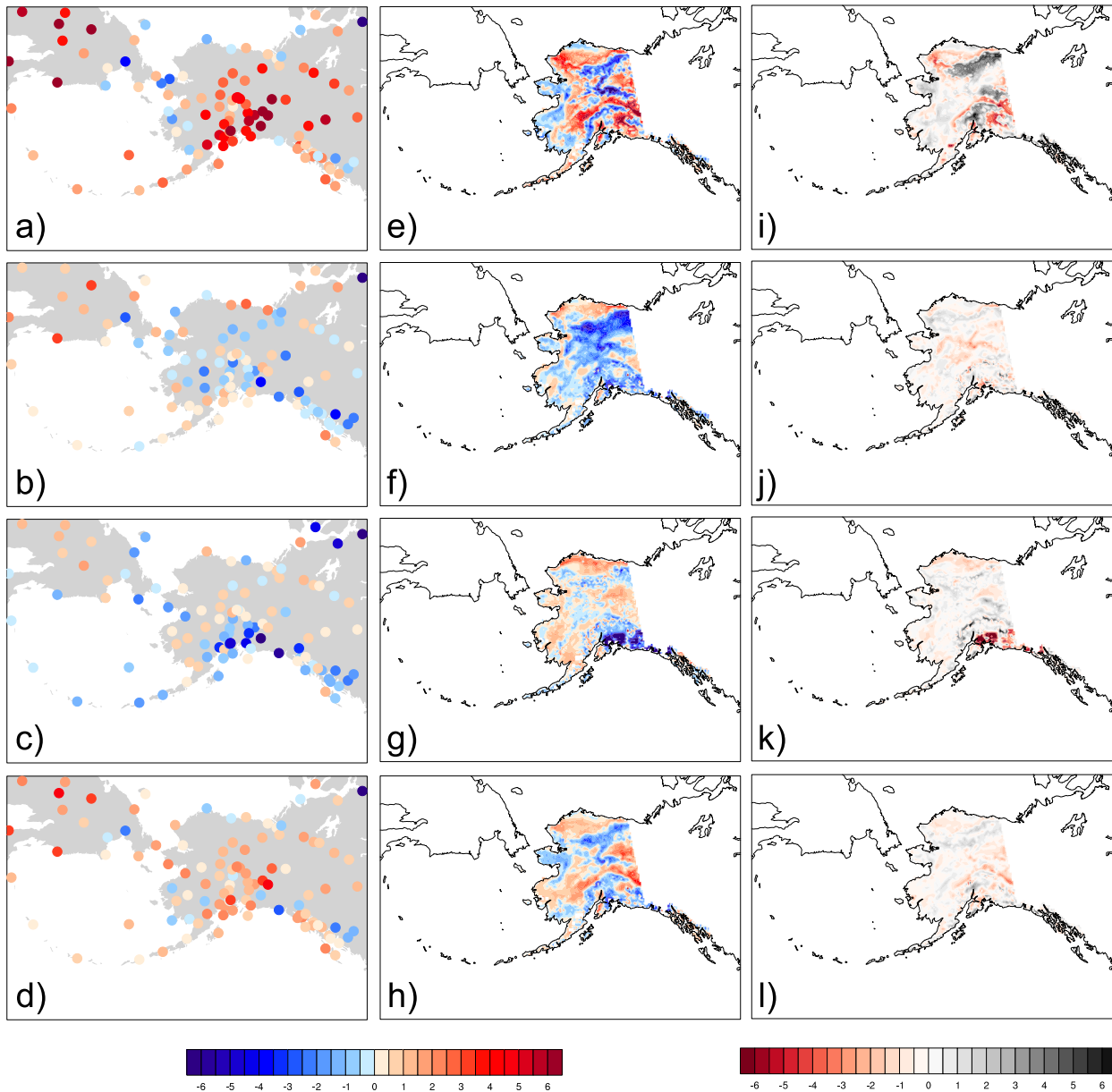


FIG. 6. (a)–(d) Downscaled minus station, (e)–(h) downscaled minus gridded observations, and (i)–(l) downscaled minus reanalysis absolute value of bias for seasonally averaged temperature ($^{\circ}\text{C}$) 1979–2009. The seasons analyzed were (top) DJF, (top middle) MAM, (bottom middle) JJA, and (bottom) SON. The station analysis in (a)–(d) was conducted at the nearest adjacent downscaled grid point to the station with the most similar elevation.

downscaled precipitation data were compared to the gridded observations, wet biases tended to be largest at higher elevations in all seasons (Figs. 7e–h), often exceeding 40 mm. The wet biases tended to be smaller in interior and northern Alaska than in coastal areas in winter, spring and fall. Biases were largest in interior and northern Alaska during the summer convection season. They were largest over higher-elevation points where they exceeded

50 mm and were smaller (in the 10–20-mm range) at lower elevations. In contrast, southeast/south-central Alaska had a substantial dry bias, with a magnitude often exceeding 50 mm, in all seasons and at all elevations when compared with the gridded observations.

Precipitation tended to have higher biases in the downscaling than the reanalysis at higher-elevation points throughout much of interior and northern Alaska

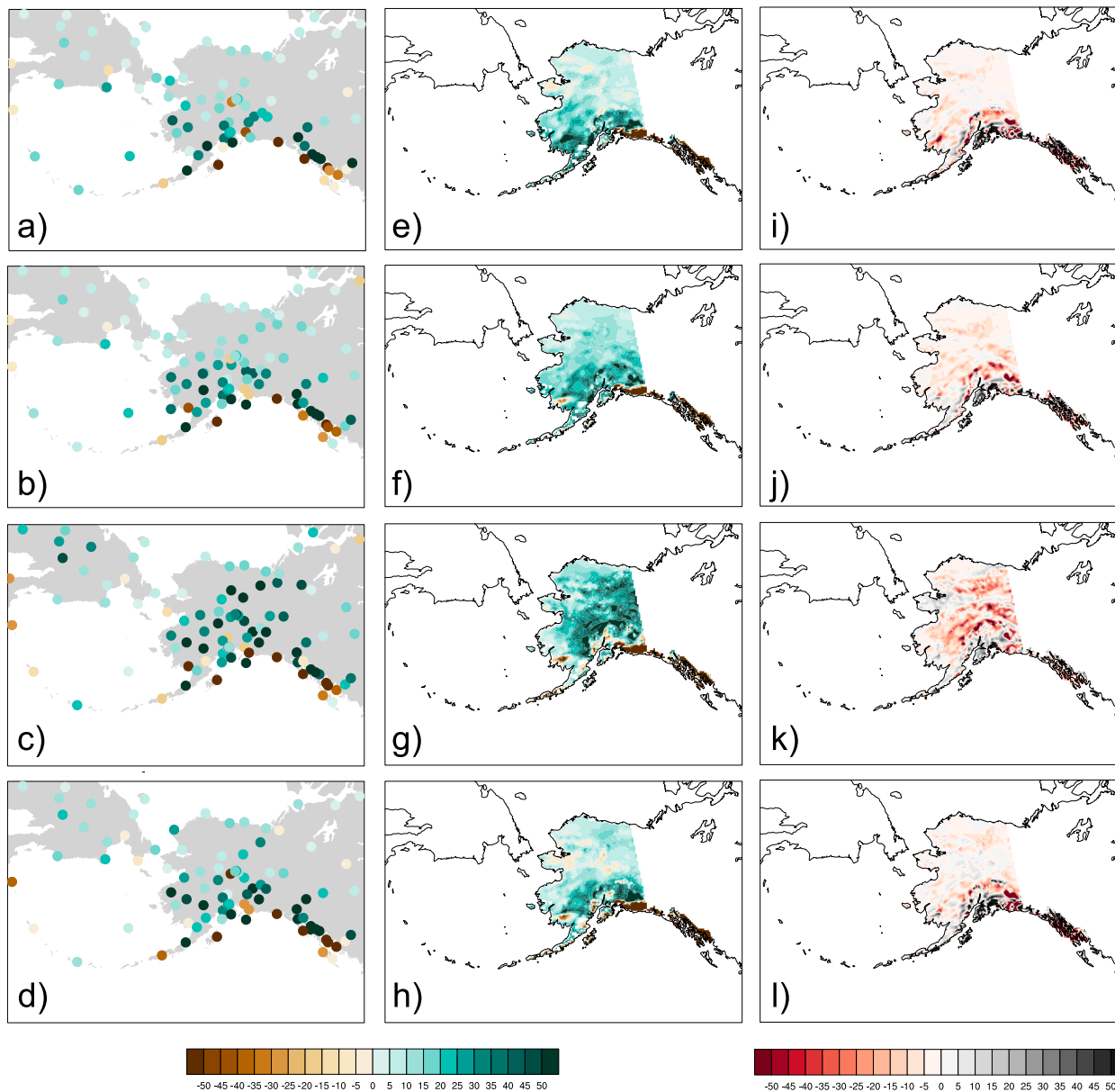


FIG. 7. As in Fig. 6, but for precipitation (mm).

(Figs. 7i–l). Precipitation biases in the interior summer were primarily larger in the downscaling compared to the reanalysis over higher-elevation terrain and were smaller at lower elevations. Southeast Alaska was an exception, and inland mountains had lower precipitation biases in the downscaling than the reanalysis in all seasons. South-central Alaska also had improved precipitation biases in the downscaling over the mountains near Anchorage and the Kenai Peninsula to the south.

Enhanced precipitation in the downscaled data is likely due to the representation of terrain in the model and possibly due to issues with the observations

themselves. For example, Fairbanks is located in a valley in interior Alaska where annual mean precipitation observed at the airport (at 135-m elevation in the valley) is about 27.4 cm, but it is 30.8 cm at a slightly higher elevation only 3 km to the north and exceeds 40 cm in the hills 20 km farther north (Shulski and Wendler 2007). Gauge undercatch is also known to be a problem in high-latitude areas where a substantial portion of the precipitation falls as snow (Goodison et al. 1998), adding uncertainty to the station observations themselves. It is also not surprising that the downscaled precipitation exceeds observational estimates, as analysis has shown

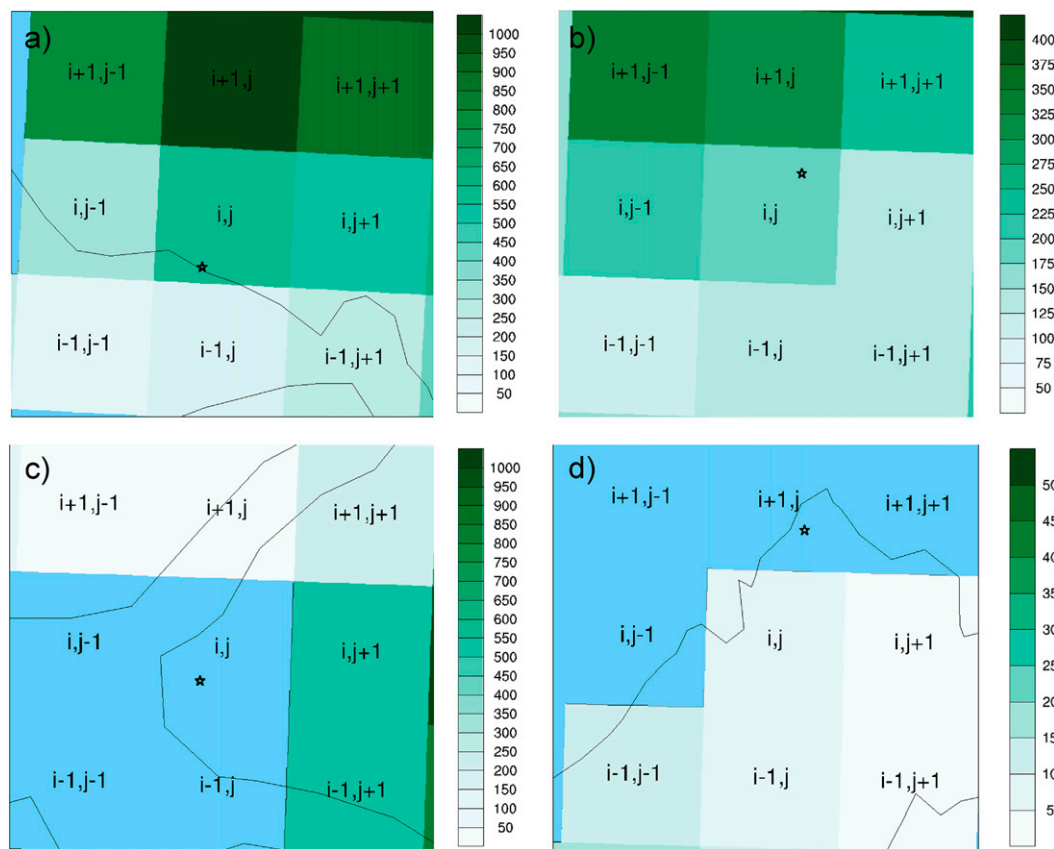


FIG. 8. The downscaled elevation for the nine grid cells surrounding the meteorological observation station at (a) Juneau, (b) Fairbanks, (c) Anchorage, and (d) Barrow. The locations of the stations are marked by a star. Elevations are in meters. Grid cells that are located over the water are shaded blue. The elevations of the stations are 7, 138, 4, and 40 m above sea level at Juneau, Fairbanks, Barrow, and Anchorage, respectively.

that ERA-Interim used as the initial, nudging, and boundary conditions for the WRF Model also has a wet bias over Alaska (Lader et al. 2016). It is again important to note that stations observations in Alaska tend to be located at lower elevations; therefore it is difficult to assess the quality of the downscaled precipitation in higher terrain. The following detailed evaluation at four of Alaska's major stations will highlight the need to carefully select which downscaled grid points should be compared to stations to help minimize local biases in temperature and precipitation.

b. Local evaluation

To better analyze the usefulness of the ERA-Interim downscaling from uniquely local perspectives and to evaluate these data over the few major population centers in Alaska, a bottom-up approach will be followed in this section. One of the goals of this exercise is to present a framework for stakeholders to understand the strengths and weaknesses of complex downscaled output and how it can be used in their backyards. Here

we will evaluate the monthly temperature and precipitation at the nearest downscaled grid cells to four cities in Alaska, together with the adjacent surrounding grid cells. The cities selected are Juneau, Fairbanks, Anchorage, and Barrow (see locations in Fig. 1a). Each city has unique topography or other features that are complicating factors. The downscaled topographies for the nine grid cells centered on each observing station are shown in Fig. 8.

Juneau is located in the coastal maritime climate of southeast Alaska. In this region of the state, precipitation amounts are high and temperatures are moderate (Bieniek et al. 2012). The topography in the vicinity of Juneau is complex, with a substantial jump in model elevation (~ 500 m) immediately north of the observation station at the airport (Fig. 8a). The elevation of the station at Juneau is 7 m, while the elevation of the nearest grid point in the downscaling is 570 m. The monthly 1979–2013 climatology temperatures at the nearest grid cell in the downscaling and the coarser reanalysis were compared to the station records (Fig. 9a).

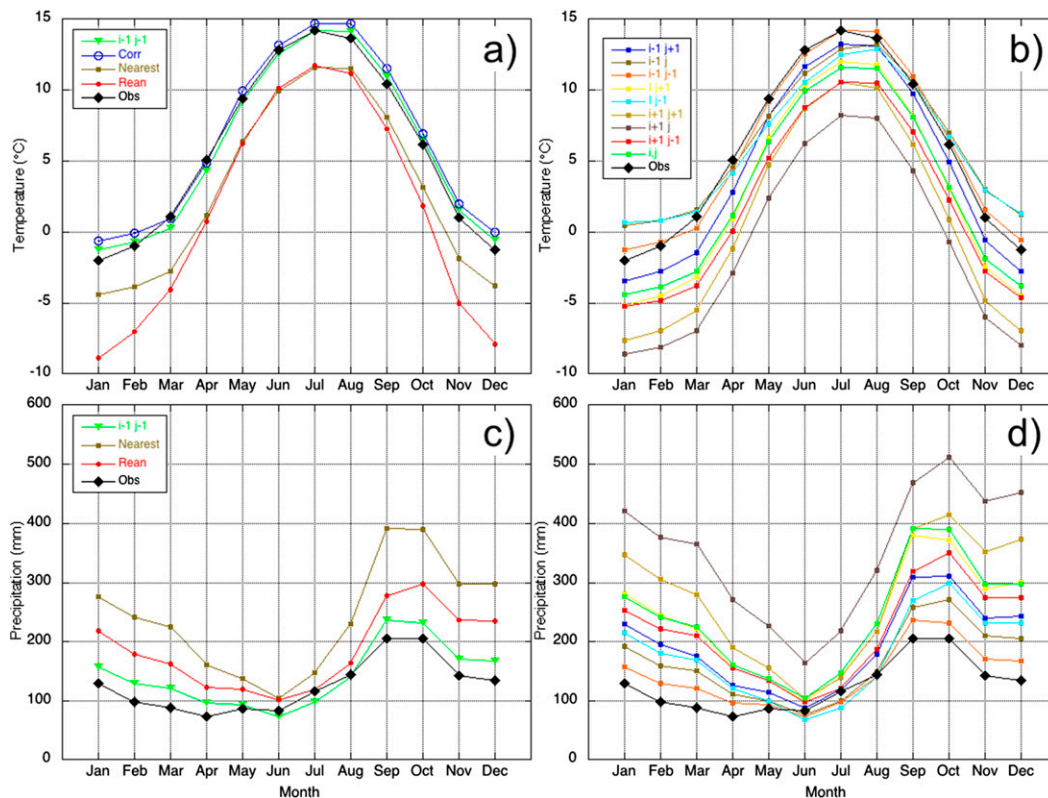


FIG. 9. Monthly 1979–2013 climatology of station observations at Juneau (black diamonds), nearest downscaled grid point to the station (brown squares), nearest downscaled grid point with most similar elevation to the station (green triangles), lapse rate corrected (open circles), and nearest reanalysis grid point (red circles) for (a) 2-m temperature and (c) precipitation. Precipitation does not include lapse-rate-corrected data. Climatology of (b) 2-m temperature and (d) precipitation at the nine grid points surrounding the station at Juneau. The line labels in (b) and (d) correspond to the grid points marked in Fig. 8a.

Both were climatologically colder throughout the year than observations at the nearest grid cell. This difference is likely due to the great variability in elevation in the Juneau region, and the temperature climatologies reflect (Fig. 9b) warmer temperatures at the lower-elevation grid cell that is more similar to the station observations. Therefore the grid cell nearest the station with the most similar elevation was compared with the observed climatology (Fig. 9a), yielding a more consistent, warmer result. A correction based on the lapse rate of the surrounding points was also carried out as a potential method to handle the elevation discrepancy between the station and the gridded data. A lapse rate was calculated each month using a least squares regression of the temperature at the nine grid cells encompassing the station shown in Fig. 8a, with temperature as the dependent variable and elevation as the independent variable. This type of regression approach has been successfully applied in various forms to calculate lapse rates in other studies (e.g., Gao et al. 2015; Li et al. 2013; Minder et al. 2010). The

lapse rate was then applied to the data at the nearest grid cell to the station using the elevation difference between that point and the station. The resulting lapse rate correction yielded a similar result to the approach with the nearest adjacent cell (Fig. 9a). Such an analysis would be more problematic for the coarser reanalysis, for which the nearest adjacent grid cells encompass a much broader geographic area than the downscaling (the nine downscaled points are within 60 km of each other, while the reanalysis points are spread over 300 km). Besides elevation, other synoptic-scale meteorological factors, such as the position of fronts and cyclones, play a greater role at the larger spatial extent of the reanalysis and may impact the derivation of local lapse rates. Therefore, the lapse rate correction could only be feasibly applied to the downscaled data.

Precipitation was also evaluated at Juneau for the downscaling and the coarse reanalysis (Fig. 9c). Both the nearest downscaled and reanalysis grid cells had higher climatological precipitation amounts than the

station observation. An evaluation of the downscaled precipitation climatologies at the surrounding grid cells reveals a large spread in the amounts of precipitation with higher amounts at higher elevations (Fig. 9d). Therefore, the nearest downscaled grid cell of similar elevation was evaluated and, while still having a wet bias, had a more favorable comparison to the data than was obtained by simply using the closest grid cell (Fig. 9c). Lapse rates for precipitation are not well defined, so no attempt was made to correct the precipitation based on lapse rates in this study.

The overestimation of precipitation at Juneau represents a local positive bias in the northern part of southeast Alaska, in contrast to the rest of southeast Alaska where the downscaling tended to be drier than gridded observations in all seasons (see Figs. 7e–h). This could be due to the somewhat blocky representation of the 20-km terrain in the WRF Model that, while more realistic than the smooth topography in the reanalysis, still does not accurately represent the pathways for upslope precipitation in this mountainous and rainy region of Alaska. Unrealistic gradients in precipitation have been noted in this region in similar WRF Model studies utilizing a 20-km grid and have been linked to the coarse terrain (Ziemen et al. 2016). For practical applications, adjustments in the gradient of precipitation may be advantageous in southeast Alaska until improvements can be made. Finer-resolution downscaling represents one approach to such improvements.

Fairbanks is located in interior Alaska and has a continental climate that is relatively dry but has a wide range of temperatures, with cold winters and warm summers (Bieniek et al. 2012). The topography around Fairbanks is somewhat hilly except on the southern side (Fig. 8b). Elevation changes are within 200–300 m in the nine grid cells being evaluated centered on the observation station located at the airport. The station at the airport is at 138-m elevation while the nearest grid cell is at 186-m elevation. While the terrain is simpler than that of Juneau, the region surrounding Fairbanks features strong temperature inversions in winter (Malingowski et al. 2014; Mayfield and Fochesatto 2013; Bourne et al. 2010). When the 1979–2013 climatology of downscaled monthly temperatures were compared with the Fairbanks station (Fig. 10a), a slight warm bias was detected in winter. This bias is likely attributable to the downscaled gridpoint elevation being higher than that of the observation site. Frequent winter temperature inversions often result in an increase in temperature with elevation in Fairbanks and temperatures can increase rapidly when moving only a few tens of meters up in elevation. The

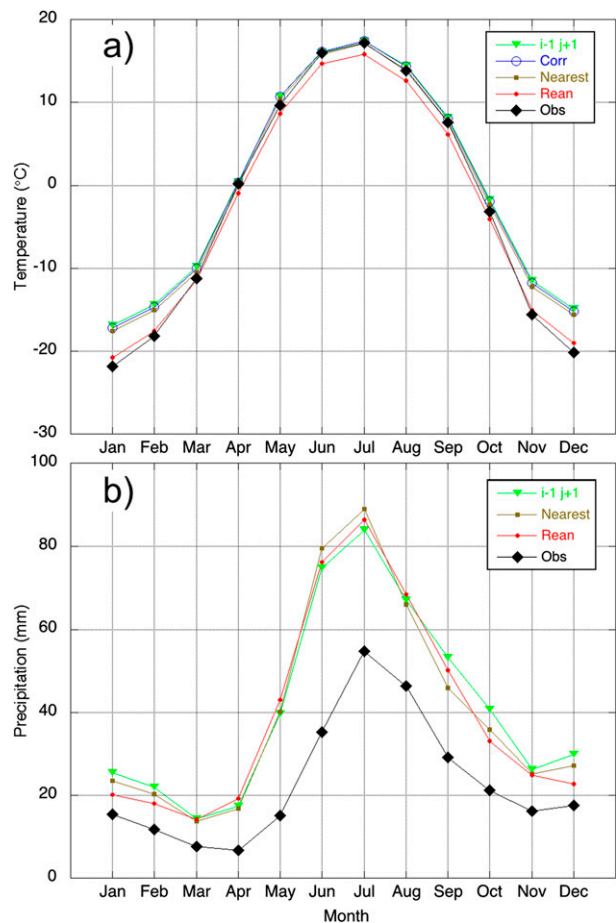


FIG. 10. Monthly 1979–2013 climatology of station observations at Fairbanks (black diamonds), nearest downscaled grid point to the station (brown squares), nearest downscaled grid point with the most similar elevation to the station (green triangles), lapse rate corrected (open circles), and nearest reanalysis grid point (red circles) for (a) 2-m temperature and (b) precipitation. Precipitation does not include lapse-rate-corrected data.

difference of nearly 50 m between the station and gridpoint elevation likely accounts for the winter warm bias. Therefore the lapse rate correction and nearest grid cell with most similar elevation approaches used in Juneau were applied to Fairbanks as a test. Neither approach reduced the winter warm bias. Fairbanks is located on the northern edge of the valley where a general warm bias was noted in winter temperatures in the previous section. The bias may therefore be due to shortcomings of the modeling system as discussed earlier. However, the downscaling performs better than the reanalysis in the warm months, both with and without any correction for elevation. The downscaled precipitation was much more similar to that of the reanalysis when compared with the observation (Fig. 10b), with both having a wet bias in all months

similar to the results of the grid-based analysis in the previous section.

Alaska's largest city, Anchorage, in south-central coastal Alaska has complex topography, especially to the east of the city (Fig. 8c) with a rise of nearly 500 m from the city's location near sea level to locations 15–20 km to the east. The station at the Anchorage airport is located at 40-m elevation. The nine downscaled grid cells that encompass the Anchorage area include four on the southwest side that are water. When the monthly downscaled temperature was compared between the grid cells and the station observation a complex story emerges (Fig. 11a). The grid cell nearest the station along with the adjacent grid cells to the west and south are over water and therefore contain a much more moderate climate than the station. In contrast, the higher-elevation grid cells over land are too cold throughout the year. The grid cells that best match the station in this case are those lower-elevation cells that are farther inland. A further complication with this location is that the adjacent waters that are present in the downscaled and reality are not resolved in the coarse reanalysis. This also precludes sea ice over the inlet in the downscaled because the inlet is not present in the reanalysis. In nature, the inlet is ice covered during much of the winter, so future downscaled efforts in this region should consider this issue. Precipitation (Fig. 11b) showed a similar elevation distribution as Juneau, with higher precipitation amounts at higher-elevation locations. However, precipitation at the nearest grid cell correlated well with that at the station.

Barrow is not a major population center but was selected for evaluation because of its location in Arctic Alaska, which has experienced significant climatic and environmental changes in recent decades (e.g., Bieniek et al. 2014; Wendler et al. 2014; Bhatt et al. 2013; Markon et al. 2012). Like Fairbanks, Barrow has a somewhat continental climate, but can be moderated when the sea ice cover is absent. Unlike the previous stations the topography in the vicinity of Barrow is quite flat with a range of only a few tens of meters (Fig. 8d). Like Anchorage, a complicating factor for selecting the nearest grid cell to the observation station is that the station is located over the ocean in the downscaled land–sea mask. Therefore the nearest grid cell over land was selected. The station and nearest downscaled grid point are both located at 4–5-m elevation, so no corrections were made to the data for elevation. The monthly 1979–2013 climatologies of temperature were compared with the station at the airport, and downscaled temperatures were found to be noticeably warmer ($\sim 2^{\circ}\text{C}$) than the observed in June–August (Fig. 12a). In contrast, reanalysis temperatures

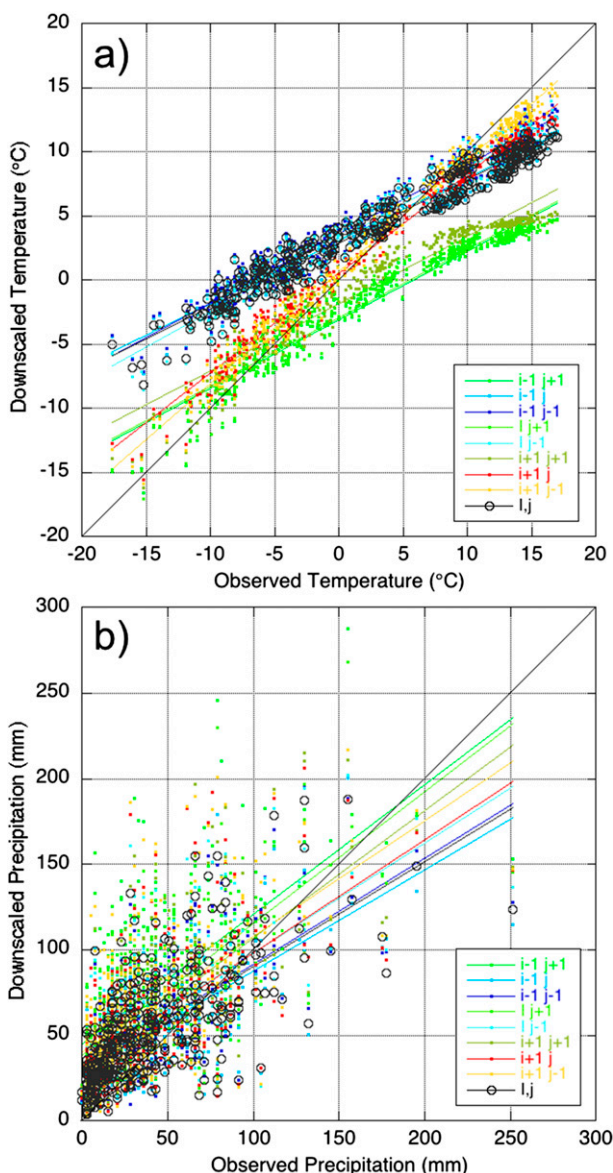


FIG. 11. Monthly (a) 2-m temperature and (b) precipitation at eight adjacent grid points vs the nearest downscaled grid point to the station at Anchorage. The 1:1 line is displayed along with the best-fit line by least squares regression for each variable. The line labels correspond to the grid points marked in Fig. 7d. The blue and green points/lines indicate water and land points respectively, and the red and yellow points/lines indicate those two grid points that have the best correlation with the Anchorage station observations.

were cooler during this same period, and no other large biases were noted during other months. The effect of cloud cover was evaluated by comparing the incoming solar radiation observed at the Barrow ARM site versus that in the WRF Model (Fig. 12b). The comparison was limited to the 1988–2013 period for which data are available from the ARM station. Based on that analysis, there is a slightly higher amount of incoming solar

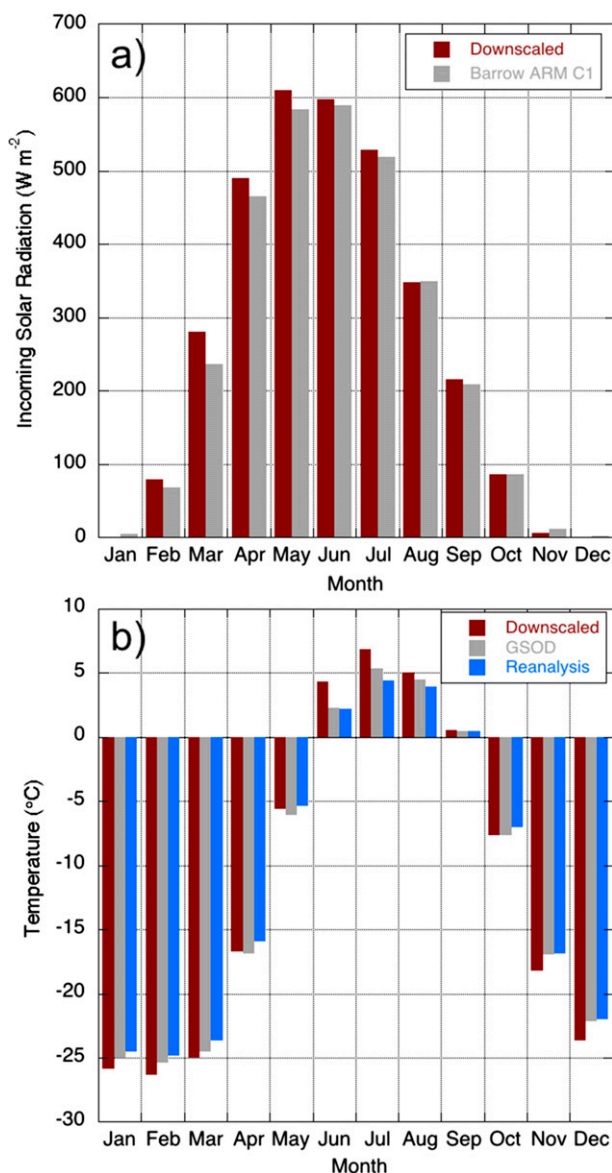


FIG. 12. Monthly (a) climatology 1979–2013 of 2-m temperature in the downscaled and ERA-Interim at the nearest grid point and the station observation at Barrow and (b) maximum daily incoming solar radiation downscaled and observed at the Barrow ARM station 1998–2013.

radiation in the WRF Model downscaling than is actually observed in May–July. However, additional factors such as sea ice are likely playing a role, and overwater fetch with the WRF Model land mask will differ from the actual fetch for various wind directions.

4. Conclusions

The results presented here show that dynamical downscaling for Alaska benefits from the higher-resolution

topography and better-resolved coastlines of a regional model such as the WRF Model. In particular, the lower temperatures and greater precipitation amounts known to characterize higher elevations are more apparent in the WRF Model output than in a coarse-resolution reanalysis such as ERA-Interim. The improved depictions of temperature and precipitation should also result in improved distributions of snow, which have already been demonstrated in regional climate model simulations for other areas such as the Pacific Northwest (Leung et al. 2003).

Because dynamical downscaling adds local information to coarser reanalysis data, it can also add local information to global model simulations for both historical and future periods. However, dynamical downscaling of global climate models will not benefit from the observational constraints on the lateral boundaries provided by forcing from a reanalysis. In the case of global climate model-derived lateral forcing, the downscaled output will be adversely impacted by any biases in the global climate model as well as any biases in the regional model (e.g., the WRF Model).

Even with the observational constraints imposed by the use of a reanalysis for boundary forcing, the biases resulting from the regional model will require corrections in many applications. For example, the use of the dynamical downscaling output to drive a glacier or land surface model will require adjustments of temperature and precipitation if biases of several degrees Celsius or several tens of a percent of precipitation are unacceptable. Since interannual variations and multidecadal changes of means have similar magnitudes, bias corrections will often be advisable, if not absolutely necessary.

The validation of the dynamically downscaled fields is problematic in a region such as Alaska where the number of high-quality surface stations with long records is only a few dozen. The locations of these stations at almost entirely low elevations and in the southern half of the state biases the station data toward higher temperatures and lower precipitation amounts. The low-precipitation bias is compounded by the tendency for gauges to undercatch precipitation by as much as 50% during the cold season. Remote sensing products offer the potential for more spatially complete validation data, although remote sensing products have their own systematic errors that may be as large as those of a regional model.

The comparison of downscaled output for data from particular observational sites highlights another challenge of model–data comparisons. Topography near sites such as Anchorage, Juneau, and even Fairbanks can vary sharply over distances comparable to the 20-km resolution of the simulation described here. A station's

location relative to a coastal boundary or a major topographic feature may not be captured even with 20-km resolution, making it necessary to maximize consistency between the station's location and the "comparison" grid cell in the WRF Model, even if maximum consistency requires the use of a WRF Model grid cell in which the station is not actually located.

Future downscaling efforts with the WRF Model in Alaska will include the use of global climate model output driven by scenarios of external forcing (greenhouse gases, aerosols) to downscale future climate changes. Downscaling of additional reanalysis products would also help to better quantify the biases in the WRF Model and the uncertainty of the downscaled output, as reanalyses have biases that vary from product to product (e.g., Lader et al. 2016). The development of bias corrections for applications to wildfire models, glacier modules, and sea ice–ocean–land interactions is also a high priority before stakeholders can fully benefit from dynamical downscaling. Finally, dynamical downscaling offers unique opportunities to address future changes in extreme events such as storms with high winds, heavy precipitation episodes, and changes in extreme temperatures over a region that is presently characterized by one of the largest annual cycles in the Northern Hemisphere.

Acknowledgments. The authors thank Nicole Mölders, Vladimir Alexeev, Richard Thoman, the two anonymous reviewers, and the editor for their fruitful discussions that helped to improve this study. Dustin Rice and Bob Torgerson provided technical support. Computational resources were provided by the Arctic Region Supercomputing Center at the University of Alaska Fairbanks. The project described in this publication was supported by Grant/Cooperative Agreement G10AC00588 from the U.S. Geological Survey. Its contents are solely the responsibility of the authors and do not necessarily represent the official views of the USGS.

REFERENCES

- Barker, D. M., and Coauthors, 2012: The Weather Research and Forecasting Model's Community Variational/Ensemble Data Assimilation System: WRFDA. *Bull. Amer. Meteor. Soc.*, **93**, 831–843, doi:10.1175/BAMS-D-11-00167.1.
- Bhatt, U. S., J. Zhang, W. V. Tangborn, C. S. Lingle, and L. Phillips, 2007: Examining glacier mass balances with a hierarchical modeling approach. *Comput. Sci. Eng.*, **9** (2), 60–67, doi:10.1109/MCSE.2007.29.
- , and Coauthors, 2013: Recent declines in warming and Arctic vegetation greening trends over pan-Arctic tundra. *Remote Sens.*, **5**, 4229–4254, doi:10.3390/rs5094229.
- Bieniek, P. A., and Coauthors, 2012: Climate divisions for Alaska based on objective methods. *J. Appl. Meteor. Climatol.*, **51**, 1276–1289, doi:10.1175/JAMC-D-11-0168.1.
- , J. E. Walsh, R. L. Thoman, and U. S. Bhatt, 2014: Using climate divisions to analyze variations and trends in Alaska temperature and precipitation. *J. Climate*, **27**, 2800–2818, doi:10.1175/JCLI-D-13-00342.1.
- Bourne, S. M., U. S. Bhatt, J. Zhang, and R. Thoman, 2010: Surface-based temperature inversions in Alaska from a climate perspective. *Atmos. Res.*, **95**, 353–366, doi:10.1016/j.atmosres.2009.09.013.
- Bromwich, D. H., A. B. Wilson, L.-S. Bai, G. W. K. Moore, and P. Bauer, 2016: A comparison of the regional Arctic System Reanalysis and the global ERA-Interim Reanalysis for the Arctic. *Quart. J. Roy. Meteor. Soc.*, doi:10.1002/qj.2527, in press.
- Dee, D. P., and Coauthors, 2011: The ERA-Interim reanalysis: Configuration and performance of the data assimilation system. *Quart. J. Roy. Meteor. Soc.*, **137**, 553–597, doi:10.1002/qj.828.
- Drusch, M., D. Vasiljevic, and P. Viterbo, 2004: ECMWF's global snow analysis: Assessment and revision based on satellite observations. *J. Appl. Meteor.*, **43**, 1282–1294, doi:10.1175/1520-0450(2004)043<1282:EGSAAA>2.0.CO;2.
- Gao, Y., J. Xu, and D. Chen, 2015: Evaluation of WRF mesoscale climate simulations over the Tibetan Plateau during 1979–2011. *J. Climate*, **28**, 2823–2841, doi:10.1175/JCLI-D-14-00300.1.
- Goodison, B. E., P. Y. T. Louie, and D. Yang, 1998: WMO solid precipitation measurement intercomparison. World Meteorological Organization Final Rep. WMO TD 872, 212 pp. [Available online at <https://www.wmo.int/pages/prog/www/IMOP/publications/IOM-67-solid-precip/WMOtd872.pdf>.]
- Grell, G., J. Dudhia, and D. Stauffer 1994: A description of the fifth generation Penn State/NCAR Mesoscale Model (MM5). NCAR Tech. Note NCAR/TN-398+STR, 121 pp., doi:10.5065/D60Z716B.
- Hill, D. F., N. Bruhis, S. E. Calos, A. Arendt, and J. Beamer, 2015: Spatial and temporal variability of freshwater discharge into the Gulf of Alaska. *J. Geophys. Res. Oceans*, **120**, 634–646, doi:10.1002/2014JC010395.
- Huang, X., and Coauthors, 2009: Four-dimensional variational data assimilation for WRF: Formulation and preliminary results. *Mon. Wea. Rev.*, **137**, 299–314, doi:10.1175/2008MWR2577.1.
- Iacono, M. J., J. S. Delamere, E. J. Mlawer, M. W. Shephard, S. A. Clough, and W. D. Collins, 2008: Radiative forcing by long-lived greenhouse gases: Calculations with the AER radiative transfer models. *J. Geophys. Res.*, **113**, D13103, doi:10.1029/2008JD009944.
- Janjić, Z., 1994: The step-mountain Eta coordinate model: Further developments of the convection, viscous sublayer, and turbulence closure schemes. *Mon. Wea. Rev.*, **122**, 927–945, doi:10.1175/1520-0493(1994)122<0927:TSMECM>2.0.CO;2.
- Knell, N. F., 2008: The reemergence of the Arctic as a strategic location. School of Advanced Military Studies, U.S. Army Command and General Staff College, 115 pp. [Available online at <http://www.dtic.mil/dtic/tr/fulltext/u2/a494394.pdf>.]
- Lader, R., U. S. Bhatt, J. E. Walsh, T. S. Rupp, and P. A. Bieniek, 2016: Two-meter temperature and precipitation from atmospheric reanalysis evaluated for Alaska. *J. Appl. Meteor. Climatol.*, doi:10.1175/JAMC-D-15-0162.1, in press.
- Leung, L. R., Y. Qian, J. Han, and J. O. Roads, 2003: Intercomparison of global reanalyses and regional simulations of cold season water budgets in the western United States. *J. Hydrometeorol.*, **4**, 1067–1087, doi:10.1175/1525-7541(2003)004<1067:IOGRAR>2.0.CO;2.

- Li, X., L. Wang, D. Chen, K. Yang, B. Xue, and L. Sun, 2013: Near-surface air temperature lapse rates in the mainland China during 1962–2011. *J. Geophys. Res. Atmos.*, **118**, 7505–7515, doi:10.1002/jgrd.50553.
- Lindsay, R., M. Wensnahan, A. Schweiger, and J. Zhang, 2014: Evaluation of seven different atmospheric reanalysis products in the Arctic. *J. Climate*, **27**, 2588–2606, doi:10.1175/JCLI-D-13-00014.1.
- Liu, F., J. R. Krieger, and J. Zhang, 2014: Toward producing the Chukchi–Beaufort High-Resolution Atmospheric Reanalysis (CBHAR) via the WRFDA data assimilation system. *Mon. Wea. Rev.*, **142**, 788–805, doi:10.1175/MWR-D-13-00063.1.
- Malingowski, J., D. Atkinson, G. J. Fochesatto, J. Cherry, and E. Stevens, 2014: An observational study of radiation temperature inversions in Fairbanks, Alaska. *Polar Sci.*, **8**, 24–39, doi:10.1016/j.polar.2014.01.002.
- Markon, C. J., S. F. Trainor, and F. S. Chapin III, Eds., 2012: The United States National Climate Assessment—Alaska technical regional report. U.S. Geological Survey Circular 1379, 148 pp. [Available online at <http://pubs.usgs.gov/circ/1379/pdf/circ1379.pdf>.]
- Mayfield, J. A., and G. J. Fochesatto, 2013: The layered structure of the winter atmospheric boundary layer in the interior of Alaska. *J. Appl. Meteor. Climatol.*, **52**, 953–973, doi:10.1175/JAMC-D-12-01.1.
- McAfee, S., G. Guentchev, and J. Eischeid, 2014: Reconciling precipitation trends in Alaska: 2. Gridded data analyses. *J. Geophys. Res.*, **119**, 13 820–13 837, doi:10.1002/2014JD022461.
- Minder, J. R., P. W. Mote, and J. D. Lundquist, 2010: Surface temperature lapse rates over complex terrain: Lessons from the Cascade Mountains. *J. Geophys. Res.*, **115**, D14122, doi:10.1029/2009JD013493.
- Mölders, N., and G. Kramm, 2010: A case study on wintertime inversions in interior Alaska with WRF. *Atmos. Res.*, **95**, 314–332, doi:10.1016/j.atmosres.2009.06.002.
- Morrison, H. C., G. Thomposn, and V. Tatarskii, 2009: Impact of cloud microphysics on the development of trailing stratiform precipitation in a simulated squall line: Comparison of one- and two-moment schemes. *Mon. Wea. Rev.*, **137**, 991–1007, doi:10.1175/2008MWR2556.1.
- Shulski, M., and G. Wendler, 2007: *The Climate of Alaska*. University of Alaska Press, 216 pp.
- Simpson, J. J., G. L. Hufford, C. Daly, J. S. Berg, and M. D. Fleming, 2005: Comparing maps of mean monthly surface temperature and precipitation for Alaska and adjacent areas of Canada produced by two different methods. *Arctic*, **58**, 137–161.
- Skamarock, W. C., and Coauthors, 2008: A description of the Advanced Research WRF version 3. NCAR Tech Note, NCAR/TN-475+STR, 113 pp, doi:10.5065/D68S4MVH.
- Soares, P. M. M., R. M. Cardoso, P. M. A. Miranda, J. de Medeiros, M. Belo-Pereira, and F. Espirito-Santo, 2012: WRF high resolution dynamical downscaling of ERA-Interim for Portugal. *Climate Dyn.*, **39**, 2497–2522, doi:10.1007/s00382-012-1315-2.
- Srivastava, P. K., D. Han, M. A. Rico-Ramirez, and T. Islam, 2013: Comparative assessment of evapotranspiration derived from NCEP and ECMWF global datasets through Weather Research and Forecasting model. *Atmos. Sci. Lett.*, **14**, 118–125, doi:10.1002/asl2.427.
- , —, —, and —, 2014: Sensitivity and uncertainty analysis of mesoscale model downscaled hydro-meteorological variables for discharge prediction. *Hydrol. Processes*, **28**, 4419–4432, doi:10.1002/hyp.9946.
- Wendler, G., B. Moore, and K. Galloway, 2014: Strong temperature increase and shrinking sea ice in Arctic Alaska. *Open Atmos. Sci. J.*, **8**, 7–15, doi:10.2174/1874282301408010007.
- Wilks, D. S., 2006: *Statistical Methods in the Atmospheric Sciences*. 2nd ed. Academic Press, 627 pp.
- Zhang, J., U. S. Bhatt, W. V. Tangborn, and C. S. Lingle, 2007a: Response of glaciers in northwestern North America to future climate change: An atmosphere/glacier hierarchical modeling approach. *Ann. Glaciol.*, **46**, 283–290, doi:10.3189/172756407782871378.
- , —, —, and —, 2007b: Climate downscaling for estimating glacier mass balances in northwestern North America: Validation with a USGS benchmark glacier. *Geophys. Res. Lett.*, **34**, L21505, doi:10.1029/2007GL031139.
- , F. Liu, W. Tao, J. Krieger, M. Shulski, and X. Zhang, 2016: Mesoscale climatology and variation of surface winds over the Chukchi–Beaufort coastal areas. *J. Climate*, doi:10.1175/JCLI-D-15-0436.1, in press.
- Zhang, X., and J. Zhang, 2001: Heat and freshwater budgets and pathways in the Arctic Mediterranean in a coupled ocean/sea-ice model. *J. Oceanogr.*, **57**, 207–237, doi:10.1023/A:1011147309004.
- , and Coauthors, 2013: Final project report for the Beaufort and Chukchi Seas Mesoscale Meteorology Modeling Study. Bureau of Ocean Energy Management, 4 pp. [Available online at <http://www.data.boem.gov/PI/PDFImages/ESPIS/5/5301.pdf>.]
- Ziemen, F., R. Hock, A. Aschwanden, C. Khroulev, C. Kienholz, A. K. Melkonian, and J. Zhang, 2016: Modeling the evolution of the Juneau Icefield between 1971 and 2100 using the Parallel Ice Sheet Model (PISM). *J. Glaciol.*, in press.